Pakistan Veterinary Journal

ISSN: 0253-8318 (PRINT), 2074-7764 (ONLINE)
DOI: 10.29261/pakvetj/2025.163

RESEARCH ARTICLE

Dose-Dependent Effects and Safety Assessment of Inactivated COVID-19 Vaccine: A Comprehensive Preclinical Study

Kivilcim Sonmez[1], Engin Alp Onen[2], Ozge Erdogan Bamac[1], Funda Yildirim[1], Srinivas Bezawada[2], Kozet Avanus[3*] and Necati Ozturk[4]

[1]Istanbul University-Cerrahpaşa Veterinary Faculty, Department of Pathology, Avcilar/Istanbul, Turkey
[2]Kocak Pharmaceuticals, Vaccine and Biotechnology R&D, Organize Sanayi Bölgesi, Kapakli/Tekirdag, Turkey
[3]Istanbul University-Cerrahpaşa Veterinary Faculty, Department of Animal Breeding & Husbandry, Avcilar/Istanbul, Turkey; [4]Istanbul University-Cerrahpasa Graduate Education Institute, Avcilar/Istanbul, Turkey
*Corresponding author: avanus@iuc.edu.tr

ARTICLE HISTORY (25-229)

Received: March 22, 2025
Revised: May 02, 2025
Accepted: May 09, 2025
Published online: May 16, 2025

Key words:
Histopathology
Inactivated SARS-CoV-2 vaccine
K18 hACE2
Transgenic mice

ABSTRACT

Currently, researchers are working to develop new vaccines against severe acute respiratory syndrome coronavirus-2 (SARS-CoV-2), causative agent of COVID-19. This study assesses the effectiveness and safety of the inactivated SARS-CoV-2 vaccine candidate KOCAK-19 in Balb/c and K18 hACE2 transgenic mice. Different groups of mice were administered varying doses of the vaccine (4µg, 6µg, and 8µg), followed by exposure to SARS-CoV-2. Utilising two distinct mouse models allowed for a thorough evaluation of both general immune responses (Balb/c) and human-like susceptibility to SARS-CoV-2 (K18 hACE2), enhancing the findings' relevance. Statistical analysis was conducted using the Kruskal-Wallis and Dunn's tests, with significance at $p<0.05$. The results emphasise the protective effects of vaccination against severe lung injury, vascular damage, and testicular atrophy. KOCAK-19 vaccination significantly decreases tracheal epithelial hyperplasia, vascular injury, perivascular lymphoid infiltration, microthrombosis, and severe haemorrhage. However, higher vaccine doses are linked to increased bronchial hyperplasia, excessive secretion, and localised inflammatory responses. The vaccinated groups showed less testicular atrophy, highlighting the vaccine's protective role in reproductive health. The study underlines optimising vaccine dosages to balance immune protection and potential adverse effects. These results offer important preclinical data to improve inactivated vaccine formulations, aiding the development of safer and more effective COVID-19 vaccination strategies.

To Cite This Article: Sonmez K, Onen EA, Bamac OE, Yildirim F, Bezawada S, Avanus K and Ozturk N, xxxx. Dose-dependent effects and safety assessment of inactivated covid-19 vaccine: a comprehensive preclinical study. Pak Vet J. http://dx.doi.org/10.29261/pakvetj/2025.163

INTRODUCTION

The COVID-19 pandemic, caused by SARS-CoV-2, has led to over 774 million cases and more than seven million deaths globally as of November 2024, profoundly impacting public health and socioeconomic stability (Bhimraj *et al.*, 2024). Vaccination remains the most effective tool to control the virus, prevent severe disease, and reduce mortality. Various COVID-19 vaccines—including mRNA-based (Pfizer-BioNTech, Moderna), viral vector (AstraZeneca), protein subunit, and inactivated virus vaccines—have been developed (Gorbalenya *et al.*, 2020; Lelis *et al.*, 2023). While many have received emergency use authorisation or full approval, concerns persist regarding their long-term safety, efficacy across populations, and effectiveness against emerging variants such as XEC, necessitating ongoing research (Nyberg *et al.*, 2021; Suthar *et al.*, 2025).

Transgenic animals, generated by introducing foreign genes, are crucial for studying pathogen-host interactions and simulating human diseases. In SARS-CoV-2 research, hACE2 transgenic mice serve as key models, replicating human infections and developing interstitial pneumonia and lung pathology like COVID-19 patients (Jiang *et al.*, 2020; Sun *et al.*, 2020; Ulbegi Polat, 2023). These models provide controlled environments to evaluate vaccine efficacy and immune responses, offering insights into protection conferred by vaccination or prior exposure. Beyond COVID-19, transgenic animals contribute to research in oncology,

In Press

neurodegenerative disorders, and autoimmune diseases, bridging the gap between preclinical and clinical studies (Patone *et al.*, 2021). However, species-specific differences necessitate comparisons with other models, such as hamsters, ferrets, mink, and non-human primates, to refine vaccine research and improve translational outcomes (Patone *et al*., 2021).

Despite effective vaccines, global immunisation efforts are hindered by vaccine hesitancy, defined as reluctance or refusal despite vaccine availability. Misinformation, safety concerns, complacency and distrust of public health institutions contribute to hesitancy (MacDonald, 2015). This reluctance undermines herd immunity, increasing the risk of outbreaks and preventable deaths. Limited preclinical data on long-term vaccine safety exacerbates these concerns. While hACE2 transgenic mice have been used to assess vaccine-induced immune responses, potential adverse effects remain underexplored. Comparing these results with findings from conventional animal models (e.g., hamsters and non-human primates) is crucial to improving translational research and refining preclinical models (Hoffmann *et al*., 2020).

This study evaluates the efficacy and side effects of experimental COVID-19 vaccines in hACE2 transgenic mice, comparing their responses to hamsters, ferrets, mink, tree shrews, and non-human primates. The experimental vaccines tested may include inactivated or attenuated viruses, viral proteins, or vectors designed to induce SARS-CoV-2 immunity. Key parameters analysed include viral replication, lung injury, inflammation, and antibody responses. This comparative approach aims to extend the understanding of immune mechanisms, refine vaccine safety profiles across models, and provide valuable insights for COVID-19 vaccine development and public health strategies.

MATERIALS AND METHODS

Our previous study on Balb/c mice focused on developing and preparing the inactivated vaccine KOCAK-19, the immunity against the vaccine in Balb/c mice, K18-hACE2 transgenic mice, and ferrets, viral loads in the lungs, trachea, and brain compared to unvaccinated controls and histopathologic alterations in Balb/c mice (Onen *et al*., 2022). This study used seven animal groups, including Balb/c and K18 hACE2 transgenic male mice (Jackson Laboratory, USA). Balb/c mice were divided into two groups: G1 (n=3) received a low virus dose without vaccination, while G2 (n=4) received a high virus dose to observe its effects on unvaccinated mice.

The transgenic mice were categorised as follows: G3 (n=11) received the virus with a 4µg vaccine dose, G4 (n=11) with a 6µg dose, and G5 (n=10) with an 8µg dose. G6 (n=10) received only the virus, and G7 (n=3) received only a 6µg vaccine dose.

The vaccine was administered on days 0 and 21. On day 35, G1 received a dose of $< 10^4$ $TCID_{50}$ live SARS-CoV-2, while G2 received $> 10^4$ $TCID_{50}$ live SARS-CoV-2 virus. Groups G3–G6 received 10^4 $TCID_{50}$ live SARS-CoV-2 virus intranasally via micropipette under negative pressure (220 Pa). All animals were sacrificed on day 45 for histopathological examination.

A routine necropsy was performed on each animal, and organ tissues were fixed in 10% formalin solution, processed for standard histopathologic examination, and embedded in paraffin blocks. 3–4 µm sections were cut using a rotary microtome (Leica, Germany), stained with haematoxylin and eosin (H&E), and examined under a light microscope (Olympus BX50, Japan). A double-blinded histopathological evaluation was conducted, with each sample scored on a 0–3 scale (0 = none, 1 = slight, 2 = moderate, 3 = severe changes). The final score was determined as the mathematical mean.

The findings obtained in the study were evaluated using the IBM SPSS Statistics 22 program for statistical analysis. The compliance of the parameters with normal distribution was assessed using the Kolmogorov-Smirnov and Shapiro-Wilks tests. In addition to descriptive statistical methods (minimum, maximum, mean, standard deviation, median) when evaluating the study data, the Kruskal-Wallis test was used to compare the parameters between groups in comparing quantitative data. Dunn's test was used to determine the group causing the difference. Significance was accepted at the $p<0.05$ level.

RESULTS

Animals: All the animals in the study survived until the sacrificial day except a few. Eight animals in G5 died overnight after receiving the vaccine, and severe congestion/haemorrhages were determined in their organs, especially the CNS and lungs, in the macroscopic evaluation of these animals. Due to rapid putrefaction, their histopathologic scores could not be determined. The mean scores of histopathological alterations found in the organs of animal groups are presented in Table 1. Distribution of histopathologic changes among groups are represented in Fig. 1 and 2.

Statistical Analysis: The suitability of the parameters for normal distribution was evaluated with Kolmogorov-Smirnov and Shapiro-Wilks tests, and it was determined that the parameters did not show normal distribution.

Histopathologic Findings

Lungs

Tracheal epithelial hyperplasia and increased secretion: A statistically significant difference was observed for tracheal epithelial hyperplasia and increased secretion (Fig. 3A and 3B) scores across the groups ($P=0.000$, $P<0.05$). Post hoc analyses revealed that the G7 had a significantly higher tracheal epithelial hyperplasia and increased secretion score than all other groups. This finding suggests that the virus alone induces severe epithelial hyperplasia and secretion, particularly in the hACE model. No significant differences were found between different groups, implying that either vaccine administration or low-dose virus exposure might mitigate this response, highlighting the potential protective effect of vaccination or lower viral load.

Perivascular lymphoid infiltrations: Perivascular lymphoid infiltration scores (Fig. 3D and 3E) significantly differed between groups ($P=0.000$, $P<0.05$). The G2 demonstrated the highest perivascular lymphoid infiltration

Table 1: Mean scores of histopathological alterations observed in the animals

Organs	Histopathology	Group 1, mice (G1) Virus (low) Vacine (-)*	Group 2, mice (G2) Virus (high) Vacine (-)*	Group 3, transgenic mice (G3) Virus (+) Vacine (4µg)*	Group 4, transgenic mice (G4) Virus (+) Vacine (6µg)*	Group 5, transgenic mice (G5) Virus (+) Vacine (8µg)*	Group 6, transgenic mice (G6) Virus (+) Vacine (-)*	Group 7, transgenic mice (G7) Virus (-) Vacine (6µg)*	PValue
Trachea and lungs (Fig. 3)	Tracheal epithelial hyperplasia and increased secretion	0.67±1.15 (0) (0-2)	0±0 (0) (0-0)	0.27±0.65 (0) (0-2)	0.73±1.1 (0) (0-3)	0±0 (0) (0-0)	2.6±0.7 (3) (1-3)	0±0 (0) (0-0)	0.000•
	Perivascular lymphoid infiltration	1.67±1.53 (2) (0-3)	2.25±0.96 (2.5) (1-3)	0.18±0.4 (0) (0-1)	0.36±0.67 (0) (0-2)	0±0 (0) (0-0)	1±1.05 (1) (0-3)	1.67±0.58 (2) (1-2)	0.004•
	Alveolitis	0±0 (0) (0-0)	0±0 (0) (0-0)	0.18±0.4 (0) (0-1)	0.18±0.6 (0) (0-2)	0±0 (0) (0-0)	0±0 (0) (0-0)	0±0 (0) (0-0)	0.714
	Hyalinisation in arterial walls	1.33±1.15 (2) (0-2)	1±1.15 (1) (0-2)	0±0 (0) (0-0)	0±0 (0) (0-0)	0±0 (0) (0-0)	0±0 (0) (0-0)	0±0 (0) (0-0)	0.001•
	Edema	1.33±1.15 (2) (0-2)	0±0 (0) (0-0)	0.09±0.3 (0) (0-1)	0.36±0.67 (0) (0-2)	0±0 (0) (0-0)	1±0.67 (1) (0-2)	0±0 (0) (0-0)	0.004•
	Hemosiderin-laden macrophages	0±0 (0) (0-0)	0±0 (0) (0-0)	0±0 (0) (0-0)	0±0 (0) (0-0)	0±0 (0) (0-0)	0.5±1.08 (0) (0-3)	0±0 (0) (0-0)	0.325
	Bronchial epithelial hyperplasia and increased secretion	0±0 (0) (0-0)	1±0 (1) (1-1)	1.91±1.04 (2) (0-3)	1.18±1.08 (1) (0-3)	3±0 (3) (3-3)	0±0 (0) (0-0)	0±0 (0) (0-0)	0.000•
	Peribronchial lymphoid infiltration	0.67±1.15 (0) (0-2)	0±0 (0) (0-0)	0.27±0.47 (0) (0-1)	0.18±0.4 (0) (0-1)	0±0 (0) (0-0)	0.7±0.82 (0.5) (0-2)	0±0 (0) (0-0)	0.303
	Hemorrhage	1.67±0.58 (2) (1-2)	0±0 (0) (0-0)	0±0 (0) (0-0)	0.36±0.81 (0) (0-2)	0±0 (0) (0-0)	0.6±1.07 (0) (0-3)	1±1 (1) (0-2)	0.009•
	Emphysema	1±1.73 (0) (0-3)	0±0 (0) (0-0)	0±0 (0) (0-0)	0.18±0.4 (0) (0-1)	0±0 (0) (0-0)	0.9±1.1 (0.5) (0-3)	1±0 (1) (1-1)	0.010•
	Alveolar macrophage infiltrations	1±1 (1) (0-2)	1.5±0.58 (1.5) (1-2)	0.18±0.4 (0) (0-1)	0.27±0.65 (0) (0-2)	0±0 (0) (0-0)	0±0 (0) (0-0)	1.67±0.58 (2) (1-2)	0.000•
	Mononuclear cell infiltrations	0.67±1.15 (0) (0-2)	1.5±0.58 (1.5) (1-2)	0.09±0.3 (0) (0-1)	0±0 (0) (0-0)	0±0 (0) (0-0)	0±0 (0) (0-0)	0±0 (0) (0-0)	0.000•
	İntraalveolar polymorph cell infiltration	0.33±0.58 (0) (0-1)	0.5±0.58 (0.5) (0-1)	0.18±0.4 (0) (0-1)	0.09±0.3 (0) (0-1)	0±0 (0) (0-0)	0±0 (0) (0-0)	1±0 (1) (1-1)	0.007•
	Interstitial pneumonia	0±0 (0) (0-0)	0.75±1.5 (0) (0-3)	0.18±0.4 (0) (0-1)	0.27±0.65 (0) (0-2)	0.5±0.71 (0.5) (0-1)	0.7±1.06 (0) (0-3)	0±0 (0) (0-0)	0.606
	Fibrinoid necrosis in small vessels	1.33±1.15 (2) (0-2)	0±0 (0) (0-0)	0±0 (0) (0-0)	0.09±0.3 (0) (0-1)	0±0 (0) (0-0)	0.2±0.42 (0) (0-1)	0±0 (0) (0-0)	0.035•
	Per diapedesis haemorrhage	0±0 (0) (0-0)	0±0 (0) (0-0)	0±0 (0) (0-0)	0±0 (0) (0-0)	0±0 (0) (0-0)	0±0 (0) (0-0)	1±0 (1) (1-1)	0.000•
	Thrombosis (micro)	0±0 (0) (0-0)	0.25±0.5 (0) (0-1)	0±0 (0) (0-0)	0.09±0.3 (0) (0-1)	0±0 (0) (0-0)	0.3±0.67 (0) (0-2)	1±0 (1) (1-1)	0.005•
	Hyperemia	1±1.73 (0) (0-3)	2.5±1 (3) (1-3)	1±1 (1) (0-3)	0.82±1.08 (0) (0-3)	1±0 (1) (1-1)	1.4±1.26 (2) (0-3)	0±0 (0) (0-0)	0.139
	Bronchiectasis	0±0 (0) (0-0)	0±0 (0) (0-0)	0±0 (0) (0-0)	0±0 (0) (0-0)	0±0 (0) (0-0)	0.2±0.63 (0) (0-2)	0±0 (0) (0-0)	0.757
	Hyaline accumulation in the bronchus	0.67±1.15 (0) (0-2)	0±0 (0) (0-0)	0±0 (0) (0-0)	0±0 (0) (0-0)	0±0 (0) (0-0)	0±0 (0) (0-0)	1.67±0.58 (2) (1-2)	0.000•
	Emphysema	0.33±0.58 (0) (0-1)	0±0 (0) (0-0)	0.09±0.3 (0) (0-1)	0±0 (0) (0-0)	0±0 (0) (0-0)	0±0 (0) (0-0)	0±0 (0) (0-0)	0.276
Nasal Sinus (Fig. 2)	Paranasal Ganglionitis and degeneration	1.33±1.53 (1) (0-3)	0.75±0.96 (0.5) (0-2)	0.64±0.67 (1) (0-2)	0.55±0.82 (0) (0-2)	0±0 (0) (0-0)	1.5±1.35 (2) (0-3)	0±0 (0) (0-0)	0.250
	Sinusitis	0.67±1.15 (0) (0-2)	0±0 (0) (0-0)	0±0 (0) (0-0)	0±0 (0) (0-0)	0±0 (0) (0-0)	0.2±0.63 (0) (0-2)	0±0 (0) (0-0)	0.260
	Increased secretion in nasal epithelia	0.67±1.15 (0) (0-2)	0±0 (0) (0-0)	0.09±0.3 (0) (0-1)	0±0 (0) (0-0)	0±0 (0) (0-0)	0±0 (0) (0-0)	0±0 (0) (0-0)	0.256
	Rhinitis	0.33±0.58 (0) (0-1)	0±0 (0) (0-0)	0±0 (0) (0-0)	0.18±0.6 (0) (0-2)	0±0 (0) (0-0)	0±0 (0) (0-0)	0±0 (0) (0-0)	0.297
CNS** (Fig. 2)	Meningeal lymphoid infiltration	0±0 (0) (0-0)	0±0 (0) (0-0)	0±0 (0) (0-0)	0.73±1.1 (0) (0-3)	0±0 (0) (0-0)	0.7±1.16 (0) (0-3)	0.67±0.58 (1) (0-1)	0.126
	Hyperplasia of choroid plexus	0±0 (0) (0-0)	0±0 (0) (0-0)	0±0 (0) (0-0)	0±0 (0) (0-0)	1.5±2.12 (1.5) (0-3)	0±0 (0) (0-0)	0±0 (0) (0-0)	0.002•
	Hyperemia	0±0 (0) (0-0)	0±0 (0) (0-0)	0±0 (0) (0-0)	0.18±0.6 (0) (0-2)	0±0 (0) (0-0)	0±0 (0) (0-0)	0±0 (0) (0-0)	0.809
	Micro thrombosis	0±0 (0) (0-0)	0±0 (0) (0-0)	0±0 (0) (0-0)	0.36±0.92 (0) (0-3)	0±0 (0) (0-0)	0±0 (0) (0-0)	0±0 (0) (0-0)	0.408
	Hemorrhage	0±0 (0) (0-0)	0±0 (0) (0-0)	0.18±0.6 (0) (0-2)	1.27±1.1 (2) (0-3)	0±0 (0) (0-0)	1.3±1.42 (1) (0-3)	0±0 (0) (0-0)	0.024•
	Perivascular lymphoid infiltrations	0.67±1.15 (0) (0-2)	0±0 (0) (0-0)	0±0 (0) (0-0)	0.09±0.3 (0) (0-1)	1±1.41 (1) (0-2)	0±0 (0) (0-0)	0±0 (0) (0-0)	0.074
	Zenker degeneration/necrosis	2.67±0.58 (3) (2-3)	2.25±0.5 (2) (2-3)	0.73±0.65 (1) (0-2)	0.55±0.69 (0) (0-2)	0±0 (0) (0-0)	2±1.15 (2) (0-3)	1.33±1.15 (2) (0-2)	0.001•
Heart (Fig. 2)	Hyalinisation in arterial walls	0±0 (0) (0-0)	0.75±0.96 (0.5) (0-2)	0±0 (0) (0-0)	0±0 (0) (0-0)	0±0 (0) (0-0)	0±0 (0) (0-0)	0±0 (0) (0-0)	0.002•
	Mononuclear cell infiltration	0.33±0.58 (0) (0-1)	0±0 (0) (0-0)	0±0 (0) (0-0)	0±0 (0) (0-0)	0±0 (0) (0-0)	0±0 (0) (0-0)	0±0 (0) (0-0)	0.034•

In Press

	Hemorrhage	0±0 (0) (0-0)	0±0 (0) (0-0)	0±0 (0) (0-0)	0±0 (0) (0-0)	0±0 (0) (0-0)	0.4±0.84 (0) (0-2)	0±0 (0) (0-0)	0.324
	Lymphoid infiltration	0±0 (0) (0-0)	0±0 (0) (0-0)	0.36±0.5 (0) (0-1)	1.18±1.08 (1) (0-3)	3±0 (3) (3-3)	0.5±1.08 (0) (0-3)	2±0 (2) (2-2)	0.004•
Abdominal lipid tissue (Fig. 3)	Abdominal fat necrosis	0±0 (0) (0-0)	0±0 (0) (0-0)	0.36±0.5 (0) (0-1)	0.73±0.9 (0) (0-2)	1.5±0.71 (1.5) (1-2)	0.1±0.32 (0) (0-1)	0±0 (0) (0-0)	0.035•
	Granuloma	0±0 (0) (0-0)	0±0 (0) (0-0)	0.45±0.82 (0) (0-2)	1.73±1.49 (3) (0-3)	0±0 (0) (0-0)	0±0 (0) (0-0)	0±0 (0) (0-0)	0.006•
	Parenchymatous degeneration	0.33±0.58 (0) (0-1)	0.5±1 (0) (0-2)	2±1.34 (3) (0-3)	1.82±1.25 (2) (0-3)	0±0 (0) (0-0)	1.7±1.34 (2) (0-3)	2.67±0.58 (3) (2-3)	0.078
	Passive congestion	0.67±0.58 (1) (0-1)	1±0.82 (1) (0-2)	0.18±0.4 (0) (0-1)	0±0 (0) (0-0)	0±0 (0) (0-0)	0±0 (0) (0-0)	0±0 (0) (0-0)	0.002•
	Focal necrosis and inflammatory cell infiltration	0±0 (0) (0-0)	0±0 (0) (0-0)	0.36±0.81 (0) (0-2)	0.18±0.4 (0) (0-1)	0±0 (0) (0-0)	0±0 (0) (0-0)	0±0 (0) (0-0)	0.635
Liver (Fig. 3)	Fatty degeneration	0±0 (0) (0-0)	0±0 (0) (0-0)	0.09±0.3 (0) (0-1)	0.18±0.4 (0) (0-1)	0±0 (0) (0-0)	0.2±0.63 (0) (0-2)	0.67±0.58 (1) (0-1)	0.211
	Hepatitis	0±0 (0) (0-0)	0±0 (0) (0-0)	0.18±0.6 (0) (0-2)	0±0 (0) (0-0)	0±0 (0) (0-0)	0.2±0.63 (0) (0-2)	0±0 (0) (0-0)	0.895
	Hemorrhage	0±0 (0) (0-0)	0±0 (0) (0-0)	0±0 (0) (0-0)	0±0 (0) (0-0)	0±0 (0) (0-0)	0±0 (0) (0-0)	0±0 (0) (0-0)	1.000
	Kupffer cell hyperplasia	0±0 (0) (0-0)	0±0 (0) (0-0)	0±0 (0) (0-0)	0±0 (0) (0-0)	0±0 (0) (0-0)	0.2±0.63 (0) (0-2)	0±0 (0) (0-0)	0.757
	Lymphoid hyperplasia	0.33±0.58 (0) (0-1)	0.5±1 (0) (0-2)	2±1.34 (3) (0-3)	1.82±1.25 (2) (0-3)	0±0 (0) (0-0)	1.7±1.34 (2) (0-3)	2.67±0.58 (3) (2-3)	0.088
	Increased plasma cell	0.67±0.58 (1) (0-1)	1±0.82 (1) (0-2)	0.18±0.4 (0) (0-1)	0±0 (0) (0-0)	0±0 (0) (0-0)	0±0 (0) (0-0)	0±0 (0) (0-0)	0.366
	Lymphoid depletion (Caryorexis)	0±0 (0) (0-0)	0±0 (0) (0-0)	0.36±0.81 (0) (0-2)	0.18±0.4 (0) (0-1)	0±0 (0) (0-0)	0±0 (0) (0-0)	0±0 (0) (0-0)	0.339
	Increased apoptosis	0±0 (0) (0-0)	0±0 (0) (0-0)	0.09±0.3 (0) (0-1)	0.18±0.4 (0) (0-1)	0±0 (0) (0-0)	0.2±0.63 (0) (0-2)	0.67±0.58 (1) (0-1)	0.002•
Spleen (Fig. 3)	Passive hyperemia	0±0 (0) (0-0)	0±0 (0) (0-0)	0.18±0.6 (0) (0-2)	0±0 (0) (0-0)	0±0 (0) (0-0)	0.2±0.63 (0) (0-2)	0±0 (0) (0-0)	0.485
	Hemosiderozis	0±0 (0) (0-0)	0±0 (0) (0-0)	0±0 (0) (0-0)	0±0 (0) (0-0)	0±0 (0) (0-0)	0±0 (0) (0-0)	0±0 (0) (0-0)	0.138
	Splenitis	0±0 (0) (0-0)	0±0 (0) (0-0)	0±0 (0) (0-0)	0±0 (0) (0-0)	0±0 (0) (0-0)	0.2±0.63 (0) (0-2)	0±0 (0) (0-0)	0.698
	Increased megakaryocytes	0.33±0.58 (0) (0-1)	0.5±1 (0) (0-2)	2±1.34 (3) (0-3)	1.82±1.25 (2) (0-3)	0±0 (0) (0-0)	1.7±1.34 (2) (0-3)	2.67±0.58 (3) (2-3)	0.416
	İnterstitial nephritis	0±0 (0) (0-0)	0±0 (0) (0-0)	0.27±0.47 (0) (0-1)	0.18±0.4 (0) (0-1)	0±0 (0) (0-0)	0±0 (0) (0-0)	0.67±0.58 (1) (0-1)	0.115
	Pyelonephritis	0±0 (0) (0-0)	0±0 (0) (0-0)	0.09±0.3 (0) (0-1)	0.09±0.3 (0) (0-1)	0±0 (0) (0-0)	0±0 (0) (0-0)	0±0 (0) (0-0)	0.915
	Tubular degeneration/ATN	0.33±0.58 (0) (0-1)	0±0 (0) (0-0)	0.09±0.3 (0) (0-1)	0.36±0.81 (0) (0-2)	1.5±2.12 (1.5) (0-3)	0.9±1.1 (0.5) (0-3)	0±0 (0) (0-0)	0.176
Kidney (Fig. 3)	Mesengial cell hyperplasia	0±0 (0) (0-0)	0±0 (0) (0-0)	0±0 (0) (0-0)	0.36±0.67 (0) (0-2)	0±0 (0) (0-0)	1.3±1.34 (1) (0-3)	0±0 (0) (0-0)	0.013•
	Hemorrhagia	0±0 (0) (0-0)	0±0 (0) (0-0)	0±0 (0) (0-0)	0.09±0.3 (0) (0-1)	0±0 (0) (0-0)	0±0 (0) (0-0)	0±0 (0) (0-0)	0.809
	Hyperemia	0±0 (0) (0-0)	0±0 (0) (0-0)	0.27±0.65 (0) (0-2)	0.73±1.1 (0) (0-3)	0±0 (0) (0-0)	0±0 (0) (0-0)	0±0 (0) (0-0)	0.206
	Membranous hyperplasia	0±0 (0) (0-0)	0±0 (0) (0-0)	0±0 (0) (0-0)	0±0 (0) (0-0)	0±0 (0) (0-0)	0.6±0.97 (0) (0-2)	0±0 (0) (0-0)	0.098
	Hemorrhagia	0±0 (0) (0-0)	0±0 (0) (0-0)	0±0 (0) (0-0)	0±0 (0) (0-0)	0±0 (0) (0-0)	0±0 (0) (0-0)	0±0 (0) (0-0)	1.000
Pancreas	Mononuclear cell infiltrations	0±0 (0) (0-0)	0±0 (0) (0-0)	0.09±0.3 (0) (0-1)	0.09±0.3 (0) (0-1)	0.5±0.71 (0.5) (0-1)	0±0 (0) (0-0)	0±0 (0) (0-0)	0.290
	Congestion	0±0 (0) (0-0)	0±0 (0) (0-0)	0±0 (0) (0-0)	0.18±0.6 (0) (0-2)	0±0 (0) (0-0)	0±0 (0) (0-0)	0±0 (0) (0-0)	0.809
	Lymphoid hyperplasia	0±0 (0) (0-0)	0±0 (0) (0-0)	0±0 (0) (0-0)	0.36±0.81 (0) (0-2)	0±0 (0) (0-0)	0±0 (0) (0-0)	0±0 (0) (0-0)	0.407
GIS***	Mediastinal lymphadenitis	0±0 (0) (0-0)	0±0 (0) (0-0)	0±0 (0) (0-0)	0.36±0.81 (0) (0-2)	0±0 (0) (0-0)	0±0 (0) (0-0)	0±0 (0) (0-0)	0.407
Testis (Fig. 3)	Atrophia	0±0 (0) (0-0)	0±0 (0) (0-0)	0±0 (0) (0-0)	0±0 (0) (0-0)	0±0 (0) (0-0)	0.9±0.74 (1) (0-2)	0±0 (0) (0-0)	0.000•

*Mean Value±Standart Deviation (medium) (min-max), **Central Nervous System, ***Gastrointestinal System, Kruskal Wallis Test •=p<0.05.

scores, considerably outpacing all vaccine-treated groups, suggesting a heightened immune response with a higher viral load, indicating that viral infection without vaccination leads to more substantial lymphoid infiltration. Similarly, the G1 had significantly higher perivascular lymphoid infiltration scores than the vaccine-treated hACE groups, further supporting the hypothesis that viral load influences lymphoid infiltration. Interestingly, there was no significant difference between the other groups, including those with varying vaccine doses. This finding implies that vaccine administration might not entirely prevent lymphoid infiltration but may reduce its severity.

Alveolitis: No significant difference in alveolitis scores (alveolitis) was observed across the groups (P=0.714, P>0.05), suggesting that alveolar inflammation did not differ significantly between viral and vaccine conditions. This might indicate that the vaccine or virus load does not

In Press

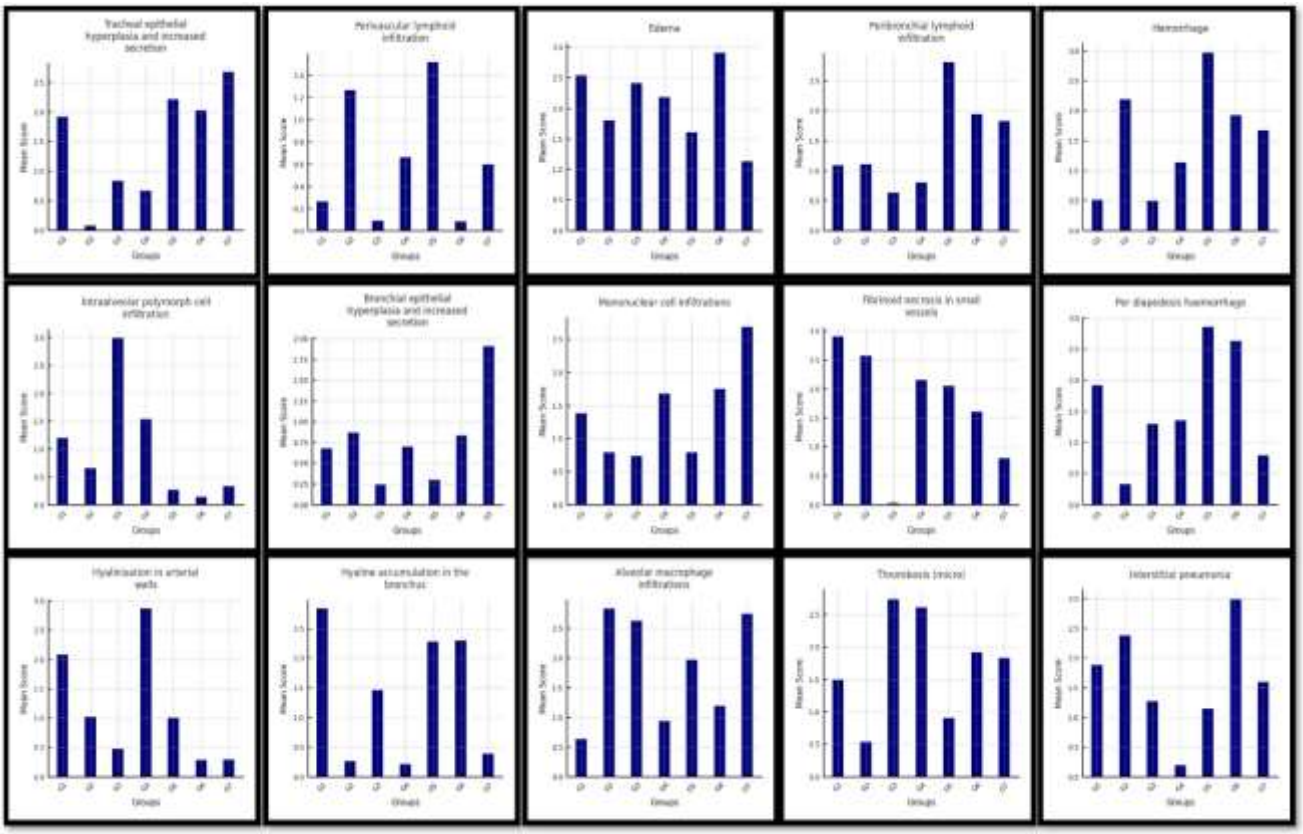

Fig. 1: Distribution of histopathologic changes in lung and trachea and lung among groups.

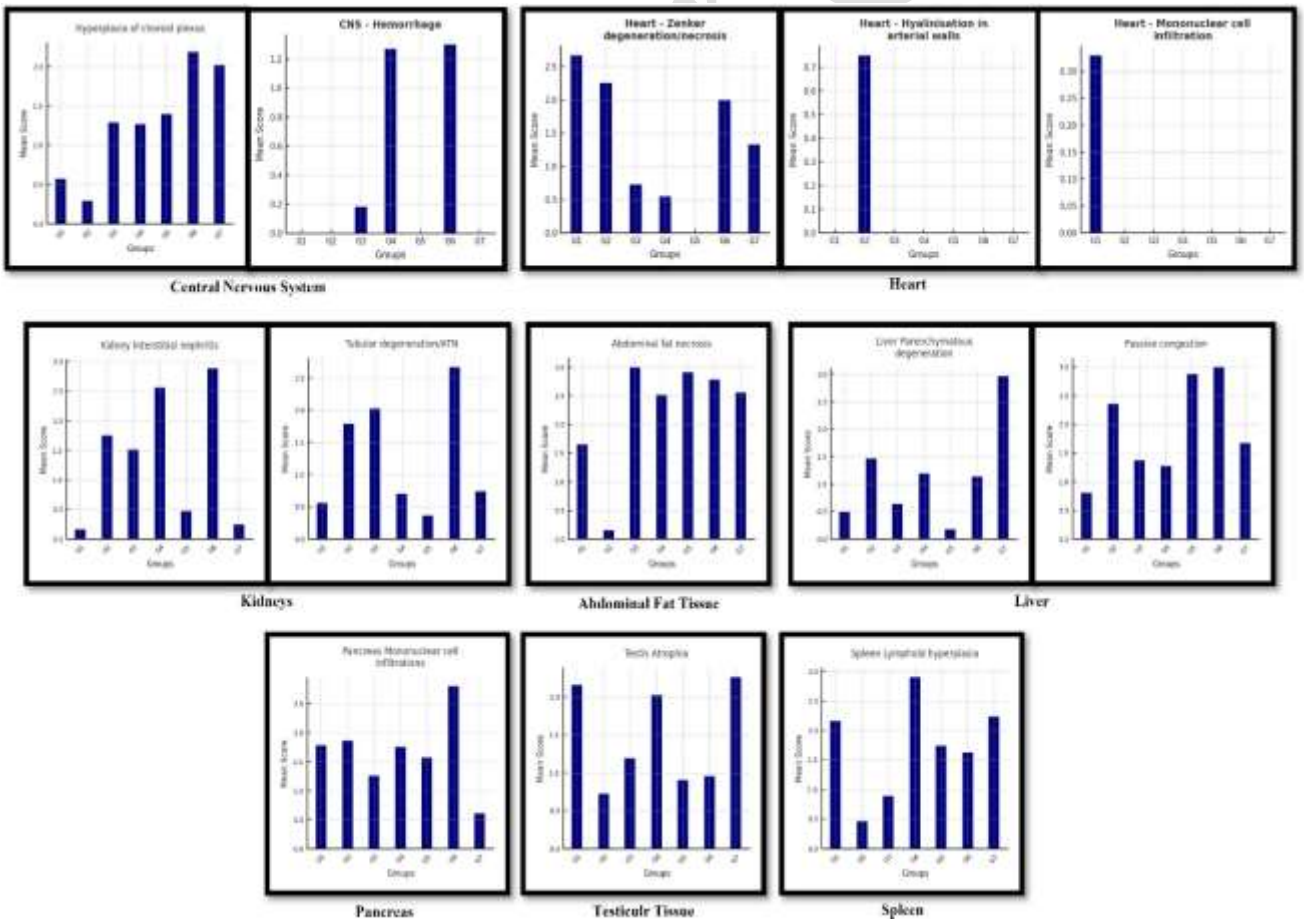

Fig. 2: Distribution of histopathologic changes in CNS, Heart, Kidneys, Abdominal Fat Tissue, Liver, Pancreas, Testicular Tissue and Spleen among groups.

heavily influence alveolar inflammation in the experimental conditions tested.

Hyalinisation in arterial walls: A significant difference was noted in arterial wall scores (P=0.001, P<0.05). G1 and G2 groups exhibited higher hyalinisation in arterial wall (Fig. 3F) scores than vaccine-treated groups, suggesting that viral infection induces more pronounced hyalinisation in arterial walls, especially without vaccination. It highlights the potential vascular damage associated with viral infection, with vaccines potentially mitigating this damage, particularly at higher doses.

Oedema: Similarly, significant differences were observed in oedema scores (P=0.001, P<0.05), with the G1 and G6 groups showing significantly higher oedema (Fig. 3F). These results suggest that both viral infection and the lack of vaccination contribute to increased oedema, which may directly result from inflammatory responses and tissue damage due to viral infection. Higher vaccine doses appear to reduce the severity of oedema, although not to the extent seen in viral-free conditions.

Bronchial epithelial hyperplasia and increased secretion: Bronchial epithelial hyperplasia and increased secretion (Fig. 3D) scores revealed significant differences (P=0.000, P<0.05), with the G5 showing the highest scores. It suggests that higher vaccine doses may exacerbate bronchial hyperplasia and secretion in the presence of the virus. The G3 and G4 also showed higher scores than several other groups, suggesting a dose-dependent effect of vaccination on bronchial hyperplasia. This could indicate an overactive immune response in the bronchial epithelium due to higher vaccine doses. This suggests further investigation to determine the optimal vaccine dose for preventing such adverse outcomes.

Haemorrhage: Significant differences in haemorrhage scores (haemorrhage) were found (P=0.009, P<0.05), with the G1 and G2 groups showing significantly higher scores than most vaccine-treated groups. This suggests that the virus, particularly at higher doses, exacerbates vascular damage and haemorrhage. Even at lower doses, vaccination appears to reduce this hemorrhagic damage, emphasising the potential protective effect of vaccines against vascular injury.

Emphysema: Emphysema (Fig. 3H) scores also showed significant differences (P=0.010, P<0.05), with G6 exhibiting the highest scores. This finding suggests that viral infection, especially without vaccination, contributes significantly to the development of emphysema. Interestingly, the G7 had a higher score than other groups, indicating that specific vaccine doses might also contribute to emphysematous changes, although to a lesser extent than viral infection.

Alveolar macrophage infiltration: The scores significantly differed between groups (P=0.000, P<0.05). The G2 had the highest infiltration, followed by the G7. This suggests that viral infection and vaccination (particularly with the 6µg dose) influence macrophage infiltration into alveolar spaces. However, the inflammatory response appears to be more pronounced with viral infection.

Per-diapedesis haemorrhage and microthrombosis: Both per-diapedesis haemorrhage (P=0.000, P<0.05) and microthrombosis (P=0.005, P<0.05) revealed significant differences. The G7 had significantly higher scores than most other groups in per diapedesis haemorrhage and micro thrombosis (Fig. 3C and 3G), indicating that the 6µg vaccine dose may promote these microvascular events. This could suggest that vaccination at specific doses may enhance inflammatory or thrombotic responses in the small vessels. However, this experimental group was too small to tell exactly.

Hyaline accumulation in the bronchi: Hyaline accumulation in the bronchi scores (P=0.000, P<0.05) showed a clear trend, with the G7 showing the highest scores, indicating that both viral exposure and the dose of the vaccine influence hyaline accumulation in the bronchial tissues. The results suggest that the vaccine, particularly at the 6µg dose, may promote this form of tissue damage, potentially due to an exacerbated immune response.

Regarding lung and tracheal differences scores, the results of this study highlight significant differences in tissue damage and inflammatory responses between groups exposed to varying combinations of virus and vaccine doses. While some vaccine doses, notably higher ones, appear to reduce specific inflammatory responses, others exacerbate tissue damage, particularly in the lungs and vasculature. These findings emphasise optimising vaccine dosages to prevent excessive immune reactions while protecting against viral-induced damage. Future studies should further explore the dose-dependent effects of vaccines and the interplay between viral infection and the host immune response.

Central Nervous System (CNS)

Meningeal lymphoid infiltration: No statistically significant differences were observed between the groups for meningeal lymphoid infiltration scores (P=0.126, P>0.05), suggesting that none of the experimental conditions, including the virus and vaccine, led to significant meningeal infiltration in the CNS. This indicates that the inflammatory responses in the meninges were either absent or similar across the groups, potentially due to the relatively localised nature of the reaction or the lack of a strong viral or immune-mediated effect in the meninges under the experimental conditions.

Hyperplasia of choroid plexus: In contrast, there was a statistically significant difference in choroid plexus scores (P=0.002, P<0.05). The G5 scored significantly higher than several other groups, including G1, G2, and various vaccine-treated hACE groups, suggesting that a higher dose of the vaccine in the presence of the virus leads to more pronounced hyperplasia in the choroid plexus. The choroid plexus hyperplasia may reflect increased immune activity and cellular proliferation in response to viral infection and an elevated vaccine dose, potentially pointing to an overactive immune response or inflammatory process within the CNS. The lack of significant differences between the other groups suggests

that lower vaccine doses or the absence of the virus do not induce as pronounced a response in the choroid plexus.

Hyperemia: Similar to the findings for meningeal lymphoid infiltration, hyperaemia (Fig. 4C-4F) scores showed no significant differences between the groups (P=0.809, P>0.05), suggesting the experimental conditions did not induce systemic vascular changes typically associated with severe inflammation or injury in the choroid plexus or other brain regions. Such modifications may occur only under different experimental setups or with more prolonged exposure durations.

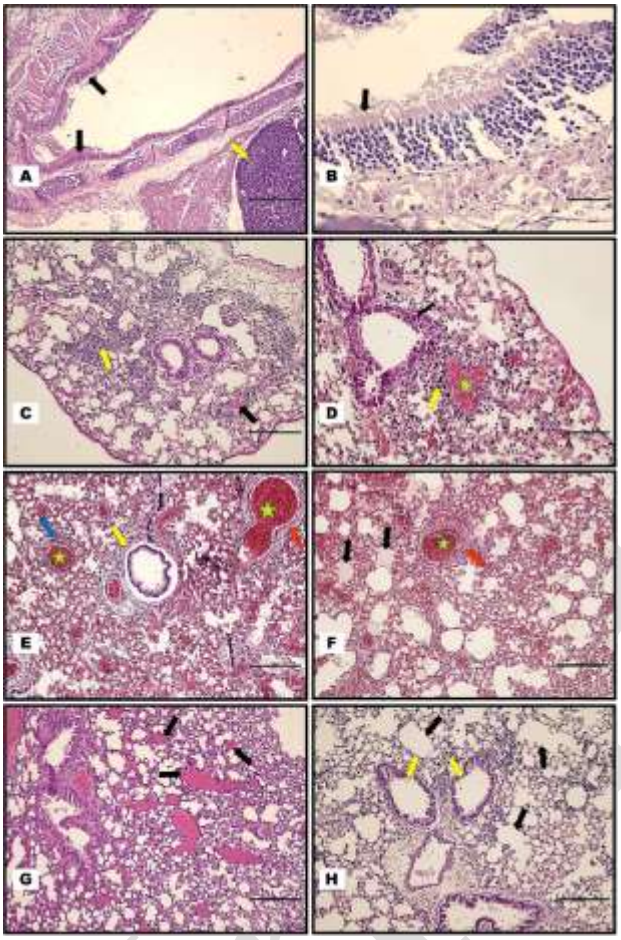

Fig. 3: Histopathologic changes in trachea and lungs, (A) Trachea: Hyperplasia of epithelial cells with increased mucus secretion (black arrow) and hyperplastic lymphoid tissue proliferation (yellow arrow). Hematoxylin-eosin (H&E) stain, scale bar = 200 µm. (B) Trachea: Close-up view showing hyperplastic epithelial cells with marked mucus secretion (black arrow). H&E stain, scale bar = 40 µm. (C) Lung: Interstitial pneumonia characterized by mononuclear cell infiltrations in the interstitial tissue (yellow arrow) and microthrombosis in small vessels (black arrow). H&E stain, scale bar = 200 µm. (D) Lung: Hyperplasia and increased secretion in bronchiolar epithelial cells (black arrow), hyperaemia (yellow asterisk), and perivascular lymphoid cell infiltrations (yellow arrow). H&E stain, scale bar = 90 µm. (E) Lung: Diffuse hyperaemia (green asterisks), perivascular lymphoid infiltrations (blue arrow), bronchiolectasis and peribronchiolitis (yellow arrow), and hyalinization of arterial walls (red arrow). H&E stain, scale bar = 200 µm. (F) Lung: Pulmonary edema characterized by interstitial fluid accumulation (black arrows) and hyalinization of arterial walls (red arrow). H&E stain, scale bar = 200 µm. (G) Lung: Presence of microthrombi within pulmonary vessels (black arrows). H&E stain, scale bar = 200 µm. (H) Lung: Emphysematous changes (black arrows) and bronchiolectasis (yellow arrows) indicating structural distortion of alveolar spaces. H&E stain, scale bar = 200 µm.

Micro thrombosis: No statistically significant difference was observed for micro thrombosis scores (P=0.408, P>0.05), suggesting that neither viral infection nor vaccination led to notable thrombotic events within the CNS under the conditions tested. These findings indicate that the inflammatory processes in the CNS while leading to other forms of tissue damage and immune responses, did not result in significant microvascular clot formation, which may be expected in more severe or chronic conditions.

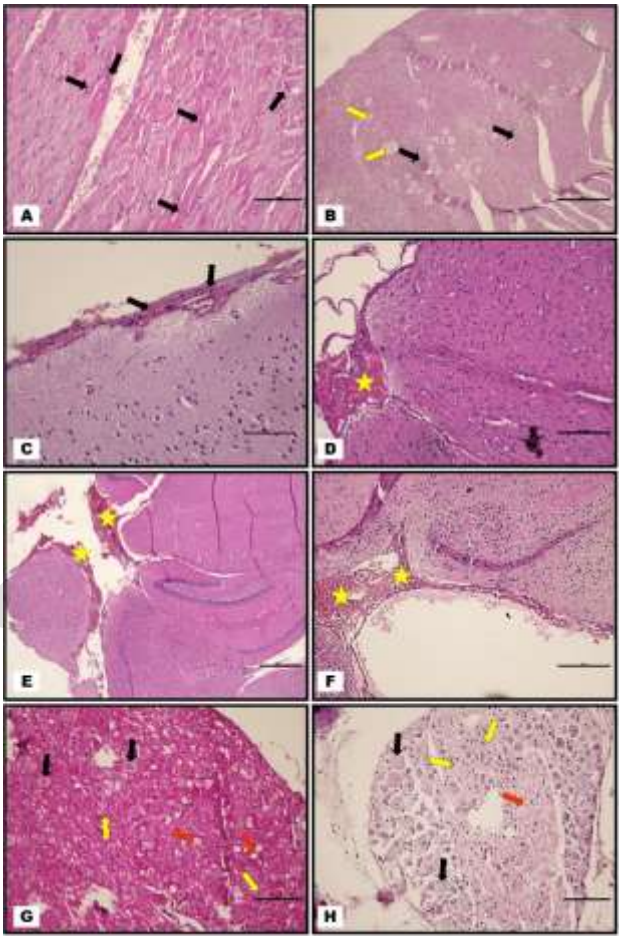

Fig. 4: Histopathologic changes in the heart, brain and nasal sinuses. (A) Heart: Extensive Zenker's degeneration in cardiac muscle fibres (black arrows). Hematoxylin-eosin (H&E) stain; scale bar = 90 µm. (B) Heart: Focal Zenker's necrosis (black arrows) and areas of muscle fiber dissolution indicative of resolving necrosis (yellow arrows). H&E stain; scale bar = 200 µm. (C) Brain: Marked hyperemia and hemorrhages in the subarachnoid space (black arrows). H&E stain; scale bar = 100 µm. (D) Brain: Subarachnoid hyperaemia and hemorrhagic foci (yellow asterisk). H&E stain; scale bar = 100 µm. (E) Brain: Widespread subarachnoid hemorrhages and vascular congestion (black arrows). H&E stain; scale bar = 400 µm. (F) Brain: Multifocal hemorrhages and intense hyperaemia in subarachnoid regions (black arrows). H&E stain; scale bar = 200 µm. (G) Nasal ganglion: Degeneration of neurons (black arrows), mononuclear inflammatory cell infiltration (yellow arrow), and neuronal dissolution (red arrows). H&E stain; scale bar = 90 µm. (H) Nasal ganglion: Neuronal degeneration (black arrows), mononuclear cell infiltration (yellow arrow), and advanced neuronal lysis (red arrows). H&E stain; scale bar = 90 µm.

Hemorrhage: In terms of haemorrhage, a statistically significant difference was found (P=0.024, P<0.05). The G4 and the G6 exhibited significantly higher haemorrhage (Fig. 4C-4F) scores than others. This suggests that both the virus

and the 6µg vaccine dose may exacerbate hemorrhagic events in the CNS, with the viral presence likely promoting vascular damage and the 6µg dose potentially intensifying this effect. The lack of significant differences between other groups implies that lower viral doses or vaccine administration at different doses (such as 4µg or 8µg) did not induce a comparable level of hemorrhagic damage. However, many animals in G5 died overnight with macroscopic findings of severe congestion/haemorrhage. This highlights the need for careful consideration of vaccine doses, as higher doses could potentially lead to more severe vascular injuries in the brain.

Perivascular lymphoid infiltrations: Perivascular lymphoid infiltrations did not show significant differences between the groups (P=0.074, P>0.05), indicating that neither viral infection nor vaccination had a marked impact on the infiltration of lymphoid cells around the blood vessels in the central nervous system (CNS). This finding contrasts with results from other literature, which reported more pronounced lymphoid infiltration. It suggests that different forms of immune activation may be more prominent in the CNS than perivascular lymphoid infiltrations or that the conditions necessary for inducing such infiltrations were unmet in this study.

Heart: Histopathologic analysis of the heart revealed significant differences in Zenker degeneration and necrosis scores (Fig. 4A and 4B). The G1, G2, and G6 groups had higher scores than those with virus and vaccine combinations, indicating that the virus alone leads to more severe degeneration.

The G2 group showed the highest scores in terms of hyalinisation in arterial walls, suggesting more pronounced changes without vaccination. The G1 group also exhibited higher mononuclear cell infiltration scores compared to others, reflecting a more excellent immune response without vaccination. No significant differences were observed in haemorrhage scores.

Abdominal Lipid Tissue

Lymphoid infiltration: There was a statistically significant difference between the groups regarding lymphoid infiltration scores (P=0.004, P<0.05). Specifically, the G5 exhibited significantly higher scores than the G1, G2, G3, and G6. Similarly, G7 also had higher scores than G1, G2, G3, and G6. The G4 also exhibited higher lymphoid infiltration than the G1 and G2. These findings suggest that vaccination, particularly with higher doses, can lead to enhanced lymphoid infiltration, possibly due to the activation of adaptive immune responses. The increase in lymphoid cells might represent an immune response to the viral infection, with vaccine doses influencing the extent of this infiltration. However, the absence of significant differences between many groups indicates that lymphoid infiltration may not always correlate with disease severity or vaccination status.

Abdominal fat necrosis: Abdominal fat necrosis (Fig. 5A) scores showed significant variation between the groups (P=0.035, P<0.05). The G5 had significantly higher scores than the G1, G2, G3, G6, and G7. The G7 also had higher scores than the G1, G2, G3, and G6. These results suggest that specific vaccination doses, particularly 8µg and 6µg, might be associated with increased abdominal fat necrosis, potentially due to immune-mediated damage. The absence of significant differences between the remaining groups implies that other factors, such as viral dose or immune activation, may influence fat necrosis independently of vaccination status.

Granuloma formation: There was also a significant difference in granuloma formation (Fig. 5B) scores (P=0.006, P<0.05). The G4 had significantly higher granuloma scores than the G1, G2, G3, G5, G6, and G7. This suggests that the 6µg vaccine dose may induce a more robust granulomatous response, possibly as part of a heightened immune reaction to the virus. Granulomas often indicate chronic inflammation, an ongoing immune response to a persistent pathogen or tissue injury. The fact that the G5 and G3 groups did not exhibit similarly high granuloma formation suggests that the immune response may vary depending on the vaccine dosage and the nature of the viral infection.

Liver

Parenchymatous degeneration and fatty degeneration: No statistically significant difference was found between the groups regarding parenchymatous degeneration (Fig. 5C) scores (P=0.078, P>0.05). Similarly, there was no statistically significant difference between the groups regarding fatty degeneration scores (P=0.211, P>0.05). This indicates that the liver's degree of parenchymal degeneration/fatty degeneration scores was relatively similar across all experimental groups, regardless of their viral infection or vaccination status. Given that the animals were kept in cages and had unlimited access to food, we concluded that the lack of exercise and the unrestricted diet contributed to the observed parenchymatous degeneration/fatty degeneration scores.

Passive congestion: In contrast, there was a statistically significant difference between the groups regarding passive congestion scores (P=0.002, P<0.05). Specifically, the G2 exhibited significantly higher scores than the G3, G4, G5, G6, and G7. The G1 also had higher scores than the G4, G5, G6, and G7. These results suggest that high viral load and the absence of vaccination may exacerbate liver congestion, potentially due to impaired blood flow or an exaggerated immune response. The notable difference between the low and high virus groups underscores the potential impact of viral load on liver congestion, while vaccination reduces this effect, especially at lower doses.

Focal necrosis and inflammatory cell infiltrations, hepatitis, haemorrhage and Kupffer cell hyperplasia: No statistically significant differences were observed between the groups regarding focal necrosis and inflammatory cell infiltration (Fig. 5D) scores (P=0.635, P>0.05). Similarly, there were no significant differences in hepatitis scores (P=0.895, P>0.05) or haemorrhage scores (P=1.000, P>0.05). This indicates that although focal necrosis, inflammatory cell infiltration, hepatitis, haemorrhage and Kupffer Cell Hyperplasia are typical responses to viral infections, these factors did not vary significantly across the groups in this study. The lack of

notable findings strongly suggests that, regardless of viral presence or vaccination, the extent of localised liver damage and the recruitment of inflammatory cells were largely unaffected by the experimental conditions. The duration of the study was relatively short, which may have influenced the outcomes.

Spleen

Lymphoid hyperplasia: There was no statistically significant difference between the groups regarding lymphoid hyperplasia scores (P=0.088, P>0.05). Lymphoid hyperplasia, which involves the enlargement of lymphoid tissue due to the activation of immune cells, did not show significant variability between the groups. This suggests that these conditions did not substantially influence lymphoid hyperplasia despite varying viral infection statuses or vaccination regimens. The immune response regarding lymphoid tissue expansion may require a more prolonged or intense immune challenge to show significant differences.

Increased plasma cells: No significant differences were observed in increased plasma cell scores (P=0.366, P>0.05). This result is consistent with the lack of a marked immune response regarding plasma cell development, suggesting that the experimental viral infections and vaccination doses did not induce strong b cell activation.

Lymphoid depletion – karyorrhexis: Similarly, there was no statistically significant difference between the groups in terms of lymphoid depletion (karyorrhexis) (Fig. 5E) scores (P=0.339, P>0.05). Lymphoid depletion is the destruction or loss of lymphoid tissue, often observed in chronic immune activation cases or viral infections. In this study, the process of lymphoid tissue depletion did not show significant differences between the experimental groups. This suggests that neither the viral infection nor the vaccination regimens caused substantial depletion of immune cells or damage to the lymphoid structures.

Increased apoptosis: In contrast to the previous markers, increased apoptosis showed a statistically significant difference between the groups (P=0.002, P<0.05). Specifically, the G2 exhibited significantly higher apoptosis scores than the G1, G3, G4, G5, G6, and G7. Increased apoptosis is often a result of excessive immune activation or viral-induced cell death, and these findings suggest that higher viral loads, combined with the absence of vaccination, may promote greater cell death in lymphoid and splenic tissues. The absence of significant differences in other groups highlights the importance of viral load in influencing immune cell apoptosis.

Passive hyperaemia and hemosiderosis: No statistically significant differences were observed between the groups regarding passive hyperaemia scores (P=0.485, P>0.05), and there was no statistically significant difference between the groups in terms of hemosiderosis scores (P=0.138, P>0.05).

Splenitis: No statistically significant differences were observed in splenitis scores (P=0.698, P>0.05), suggesting that viral infection or vaccination did not markedly affect splenic tissue, at least not in gross inflammatory changes.

Increased megakaryocytes: There was no statistically significant difference between the groups regarding increased megakaryocyte (Fig. 5E) scores (P=0.416, P>0.05).

The lack of significant differences in markers such as Lymphoid hyperplasia, increased plasma cell, lymphoid depletion, Passive hyperaemia and hemosiderosis, Splenitis, and Increased Megakaryocytes suggests that the experimental conditions did not substantially affect immune activation and haematological responses. This could indicate that the viral infections and the varying vaccination doses did not significantly impact the proliferation of immune cells, iron accumulation, or megakaryocyte activity in these tissues or that the duration of the experimental design was too short to demonstrate the changes.

Kidneys

Interstitial nephritis and pyelonephritis: There were no statistically significant differences regarding interstitial nephritis scores (P=0.115, P>0.05). Similarly, there was no statistically significant difference between the groups regarding pyelonephritis (Fig. 5F) scores (P=0.915, P>0.05).

Tubular degeneration/acute tubular necrosis – ATNs: The scores for Tubular degeneration/ATNs (Fig. 5F) also showed no statistically significant differences between groups (P=0.176, P>0.05). The lack of considerable variation in the presented study suggests that the viral infection and vaccination protocols did not result in significant renal tubular damage or degeneration, indicating that kidney function and structure were largely preserved.

Mesangial cell hyperplasia: Mesangial cell hyperplasia showed a statistically significant difference between the groups (p=0.013; P<0.05). Specifically, the G6 exhibited significantly higher scores compared to the G1, G2, G3, G4, G5, and G7 (P<0.05). The significantly higher scores suggest that the absence of vaccination with viral infection may have increased mesangial cell proliferation, reflecting a more pronounced immune response or immune-mediated kidney injury in this group.

Haemorrhage and hyperaemia: No statistically significant differences were observed in haemorrhage scores (p=0.809, P>0.05). This finding suggests that viral infection or vaccination did not lead to substantial blood vessel rupture or internal bleeding in the kidneys.

Similarly, hyperaemia showed no statistically significant differences between the groups (P=0.206, P>0.05).

Membranous hyperplasia: Membranous hyperplasia did not show significant differences between groups (P=0.098, P>0.05). The lack of substantial differences suggests that the experimental conditions did not alter glomerular membranes, which may imply that the immune responses or viral infection did not cause significant glomerular damage.

Nasal Sinuses

Paranasal ganglionitis and degeneration: There was no statistically significant difference between the groups regarding paranasal ganglionitis and degeneration (Fig. 4G

and 4H) scores (P=0.250, P>0.05). The lack of significant differences across the groups suggests neither the viral infections nor the vaccination doses resulted in paranasal ganglion inflammation or degeneration. This finding may indicate that the experimental conditions did not heavily impact the paranasal ganglia, highlighting this study's relatively localised nature of the viral infections.

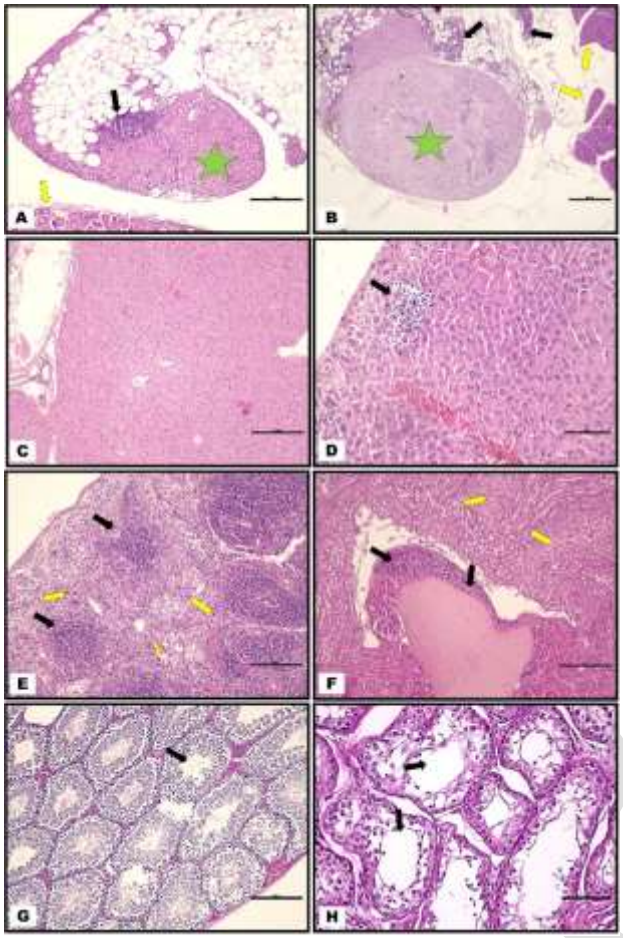

Fig. 5: Histopathologic changes in abdominal lipid tissue, liver, spleen, kidneys and testis. (A) Abdominal adipose tissue: Fat necrosis (green asterisk) with mononuclear inflammatory cell infiltration (black arrow). Adjacent renal tissue is visible (yellow arrow). Hematoxylin-eosin (H&E) stain; scale bar = 200 µm. (B) Abdominal adipose tissue: Granulomatous lesion (green asterisk) accompanied by mononuclear infiltrates (black arrow). Nearby pancreatic tissue is indicated (yellow arrow). H&E stain; scale bar = 400 µm. (C) Liver: Extensive parenchymatous degeneration with granular cytoplasmic changes in hepatocytes. H&E stain; scale bar = 200 µm. (D) Liver: Focal hepatic necrosis with mononuclear inflammatory infiltration (black arrow). H&E stain; scale bar = 90 µm. (E) Spleen: Lymphoid depletion with hyalinization (black arrows) and increased megakaryocyte presence (yellow arrows). H&E stain; scale bar = 200 µm. (F) Kidney: Mononuclear cell infiltrates within the renal pelvis (black arrows) and acute tubular necrosis (yellow arrows). H&E stain; scale bar = 200 µm. (G) Testis: Moderate degeneration characterized by disorganization of the germinal epithelium and sloughing of seminiferous epithelium into the lumen, despite abundant spermatozoa (black arrow). H&E stain; scale bar = 200 µm. (H) Testis: Severe testicular degeneration with loss of spermatogenesis; only few spermatocytes remain, with absence of spermatids and spermatozoa (black arrow). H&E stain; scale bar = 90 µm.

Sinusitis: Similarly, sinusitis scores did not show a statistically significant difference between the groups (P=0.260, P>0.05). Suggesting that the viral infections and vaccination regimens did not induce substantial inflammatory changes within the sinus cavities and pointing to minimal involvement of the sinuses in the observed responses.

Increased secretion in nasal epithelia: No statistically significant differences were observed in increased secretion (P=0.256, P>0.05). This result suggests that the experimental conditions, including viral exposure and vaccination, did not lead to noticeable changes in nasal secretion levels. As such, the findings imply that the nasal epithelium did not undergo significant functional alterations or secretion responses during the study.

Rhinitis: Rhinitis scores also showed no statistically significant differences between the groups (P=0.297, P>0.05). No substantial changes in rhinitis were observed across the groups, indicating that the viral infections and vaccine treatments did not induce considerable inflammation in the nasal passages.

Pancreas

Haemorrhage, mononuclear cell infiltrations, and congestion: There was no statistically significant difference between the groups regarding haemorrhage scores (P=1.000, P>0.05). Similarly, there was no statistically significant difference between the groups regarding mononuclear cell infiltration scores (P=0.290, P>0.05). Regarding congestion, no statistically significant differences were observed between the groups (P=0.809, P>0.05).

Gastrointestinal Track

Lymphoid hyperplasia and mediastinal lymphadenitis: Both lymphoid hyperplasia and mediastinal lymphadenitis scores showed no statistically significant difference between groups (P:0.407, P>0.05). This suggests that the experimental conditions or treatments had no measurable effect on these gastrointestinal parameters.

Testicular tissue

Atrophy: A statistically significant difference was observed between groups for atrophy (Fig. 5G and 5H) scores (p: 0.000, P<0.05). The G6 showed higher scores compared to all groups. No significant differences were observed between the other groups (P>0.05), suggesting that mice with hACE without vaccination are much more susceptible to testicular atrophy in the presence of infection. Groups with vaccination (4 µg, 6 µg, and 8 µg doses) showed lower atrophic scores, suggesting that the significant results highlight the potential impact of viral infection on testicular health and the protective role of vaccination. These findings are particularly relevant in viruses that target reproductive tissues (e.g., SARS-CoV-2, Zika) (Guo *et al*. 2024; Javadzahed *et al*. 2024).

DISCUSSION

The findings of this study offer significant insights into the immune responses and safety profiles of experimental anti-COVID-19 vaccines in transgenic and conventional animal models. K18 hACE2 mice demonstrated unique susceptibilities and immune responses compared to other models, emphasising the importance of species-specific considerations in preclinical vaccine research (Muñoz-Fontela *et al*., 2020).

The reduction in tracheal epithelial hyperplasia and vascular damage in vaccinated groups underscores the protective role of vaccination against severe pulmonary injury. These observations align with earlier studies demonstrating the efficacy of vaccines in reducing SARS-CoV-2-induced lung pathology in animal models (Sun *et al*., 2020; Jiang *et al*., 2020). However, the higher incidence of bronchial epithelial hyperplasia and secretion in groups receiving higher vaccine doses suggests a dose-dependent exacerbation of immune responses. This phenomenon has been noted in studies exploring hyperactive immune responses to mRNA and viral vector vaccines, particularly at higher doses (Hoffmann *et al*., 2020; Bhimraj *et al*., 2024). Notably, preclinical evaluations of mRNA vaccines like BNT162b2, mRNA-1273 and GLB-COV2-043 have shown dose-dependent inflammatory responses in rhesus macaques, highlighting the need for optimised vaccine formulations (Vogel *et al*., 2021; Corbett *et al*., 2020, Lelis *et al*., 2023).

The observed vascular abnormalities, including perivascular lymphoid infiltration, microthrombosis, and hemorrhagic damage, were significantly mitigated in vaccinated groups compared to unvaccinated ones. These findings are consistent with reports of reduced vascular injury in vaccinated animal models due to the attenuation of the cytokine storm and endothelial damage associated with SARS-CoV-2 infection (Nyberg *et al*., 2021; Guebre-Xabier *et al*., 2020). However, the increased per diapedesis haemorrhage and microvascular thrombosis in certain vaccinated groups (e.g., G7) suggest optimising vaccine doses to balance immune activation and vascular safety (Yu *et al*., 2020; Liu *et al*., 2022).

The CNS findings, particularly the hyperplasia of the choroid plexus in high-dose vaccine groups, raise concerns about potential neuroinflammatory effects. These results corroborate earlier findings that suggest SARS-CoV-2 infection and vaccination can elicit CNS immune activation, albeit in varying degrees depending on dose and viral exposure (Guo *et al*., 2024; Javadzadeh *et al*., 2024). Additionally, studies on animal models have highlighted the role of SARS-CoV-2 in inducing neurological inflammation, though such effects are less pronounced in vaccinated subjects (Chen *et al*., 2024).

The marked reduction in testicular atrophy among vaccinated groups highlights the vaccine's protective role against SARS-CoV-2-induced reproductive damage. Previous literature has documented the virus's tropism for reproductive tissues, leading to testicular inflammation and impaired fertility in males (Guo *et al*., 2024). Our findings further underscore the necessity of vaccination in mitigating these adverse effects, as confirmed by studies demonstrating the preservation of reproductive health in vaccinated animal models (Lu *et al*., 2024).

Similarly, the absence of significant differences in liver and renal pathology across most groups, except for passive congestion in the liver, suggests that both viral infection and vaccination exert limited direct effects on these organs under experimental conditions. These findings are consistent with other preclinical studies where systemic inflammation was observed to cause transient hepatic and renal changes, which were generally mild in vaccinated subjects (Patone *et al*., 2021; Bhimraj *et al*., 2024).

The K18-hACE2 transgenic mouse model has been extensively used in COVID-19 vaccine research for its ability to replicate both mild and severe SARS-CoV-2 infections (Winkler *et al*., 2020; Oladunni *et al*., 2020). Previous studies reported severe histopathological findings, including diffuse alveolar damage, interstitial pneumonia, vascular congestion, microthrombosis, and neuroinvasion in unvaccinated animals (Fan *et al*., 2022; Yinda *et al*., 2021). Additionally, vaccine-induced inflammatory responses have been observed in infected animals (Wu *et al*., 2021). Consistent with the literature, our study found significant organ damage in the lungs, brain, heart, liver, and testes of unvaccinated groups (G2, G6). In contrast, animals vaccinated with the inactivated vaccine at doses of 4 µg and 6 µg exhibited significantly reduced lesion severity, such as interstitial pneumonia, perivascular lymphocyte infiltration, Zenker degeneration, and hepatic congestion ($P<0.05$). These findings highlight the vaccine's efficacy in mitigating systemic damage and achieving a balanced safety and immune profile, especially at the 4 µg and 6 µg doses. Previous studies, including Kruglov *et al*. (2024) and Fumagalli *et al*. (2022), demonstrated the immunogenicity and viral load control of inactivated vaccines but focused only on pulmonary and neurological impacts. Giannakopoulos *et al*. (2023) reported testicular damage associated with SARS-CoV-2 infection but did not assess the protective effects of vaccination. Unlike these studies, ours uniquely provides comprehensive histopathological data across multiple organ systems, including testicular degeneration and local vaccine reactions. This study fills critical gaps in the literature by extending beyond pulmonary and neurological damage reported in prior studies (Fan *et al*., 2022; Yinda *et al*., 2021; Oladunni *et al*., 2020). For the first time, testicular degeneration, cardiovascular damage, splenic hyalinization, and local vaccine reactions are evaluated in-depth, demonstrating the systemic protective effects of the inactivated vaccine. These findings emphasize the importance of broad histopathological assessments in preclinical vaccine studies, offering valuable insights into the safety and efficacy profiles of vaccines.

In a phase 1/2 clinical study conducted by Zhang *et al*. (2020), 3µg and 6µg doses of Sinovac inactivated SARS-CoV-2 vaccine were shown to be safe and effective with a two-dose (14 days apart) administration protocol. In line with this literature, 4µg and 6µg doses were selected in our study to provide an optimal immune response and safety profile. In addition, the 8µg dose was used to evaluate the potential side effects of higher dose applications and to determine safety margins. Thus, it was aimed to determine the most appropriate dose range in terms of both efficacy and safety (Zhang *et al*., 2020). While the study confirms the overall protective effects of vaccination against SARS-CoV-2, the dose-dependent adverse effects, particularly in higher vaccine doses where nearly all animals in the high-dose group (G5) died overnight after receiving the vaccine, warrant further investigation. Future research should focus on dose optimisation to identify the minimal effective dose that elicits robust immune protection while minimising adverse effects. Long-term studies are also needed to assess the chronic effects of vaccination and SARS-CoV-2 infection on systemic and organ-specific health. Expanding the comparative analysis to other animal models, such as

non-human primates, will further enhance the translational relevance of these findings (Muñoz-Fontela *et al*., 2020; Munshi *et al*., 2021; Chen *et al*., 2024).

Additionally, highlighting preclinical safety data is essential to address vaccine hesitancy. Transparent reporting of potential side effects, alongside protective benefits, can bolster public confidence in vaccination campaigns (MacDonald, 2015).

Inactivated SARS-CoV-2 vaccines provide more balanced protection against variants by inducing a broad immune response not only against the spike protein but also against other structural proteins of the virus (Li *et al*., 2021). Inactivated vaccines such as Sinovac have met high safety standards by offering a low systemic side effect profile and strong humoral responses and have enabled safe use in large populations (Zhang *et al*., 2021). Their ability to be stored under standard cold chain conditions such as 2–8 °C has created a significant logistical advantage, especially for low- and middle-income countries (Zhang *et al*., 2021). In addition, a two-dose vaccination protocol administered at 14–28 days provided optimal protection by maximising the immune response (Zhang *et al*., 2021; Tanriover *et al*., 2021). The significant and sustained increase in antibody levels and T-cell responses obtained with the third dose application shows that inactivated vaccines also provide long-term immunity (Lelis *et al*., 2023). However, the current study is limited to a 45-day follow-up period and may not fully evaluate late-onset adverse effects or long-term immunity levels. Therefore, it is important to conduct future, longer-term follow-up studies to understand better the long-term efficacy and safety profiles of inactivated vaccines.

This study underscores the importance of preclinical models in understanding vaccine efficacy and safety. While vaccination demonstrates clear protective benefits against SARS-CoV-2-induced pathology, dose-dependent adverse effects highlight the need for cautiously optimising vaccination strategies. All data obtained from the presented study demonstrate that inactivated vaccines are not only a temporary option in global vaccination but a sustainable and strategic solution. These findings contribute to the broader understanding of vaccine responses and inform the development of safer, more effective COVID-19 vaccines. Some groups had very small animal populations due to factors such as sudden deaths, which led to an imbalanced distribution among groups and may have affected the statistical evaluations. Future studies with larger and more evenly distributed animal groups are recommended to allow for more robust and comprehensive analyses of the findings.

Ethical declaration: All procedures were approved by the Animal Local Ethics Committee of Kocak Pharmaceuticals (Approval No: 2020-5) and conducted in line with national welfare standards. Animals were monitored twice daily for health and behaviour. Humane endpoints and appropriate analgesia, anaesthesia, and euthanasia methods were used to minimise suffering.

Contribution of authors: Vaccination development, experimental design, and applications are performed by Engin Alp Onen and Srinivas Bezawada. Kivilcim Sonmez, Ozge Erdogan Bamac, and Funda Yildirim performed necropsies and macroscopic examinations. Necati Ozturk performs tissue processing, sectioning and staining. Kivilcim Sonmez, Ozge Erdogan Bamac, and Funda Yildirim performed histopathologic examinations and scoring. Kozet Avanus provided statistical analyses and information on transgenic animals. Kivilcim Sonmez, Kozet Avanus and Necati Ozturk performed micro photography and manuscript editing. For English editing, Grammarly premium edition version 1.2.141.1617 is used.

REFERENCES

Bhimraj A, Morgan RL, Hirsch SA, *et al*., 2024. Infectious Diseases Society of America guidelines on treating and managing patients with COVID-19. Clin Infect Dis, ciae435.

Chen Z, Yuan Y, Hu Q, *et al*., 2024. SARS-CoV-2 immunity in animal models. Cell Mol Immunol 21: 119–133.

Corbett KS, Flynn B, Foulds KE, *et al*., 2020. Evaluation of the mRNA-1273 vaccine against SARS-CoV-2 in non-human primates. NEJM 383(16): 1544–1555.

Fan C, Wu Y, Rui X, *et al*., 2022. Animal models for COVID-19: advances, gaps and perspectives. Sig Transd Targ Ther 7(1): 220.

Fumagalli V, Ravà M, Marotta D, *et al*., 2022. Administration of aerosolized SARS-CoV-2 to K18-hACE2 mice uncouples respiratory infection from fatal neuroinvasion. Sci Immunol 7: eabl9929.

Giannakopoulos S, Strange DP, Jiyarom B, *et al*., 2023. In vitro evidence against productive SARS-CoV-2 infection of human testicular cells: Bystander effects of infection mediate testicular injury. PLoS Pathog 19(5): e1011409.

Gorbalenya AE, Baker SC, Baric RS, *et al*., 2020. The species severe acute respiratory syndrome-related coronavirus: Classifying 2019-nCoV and naming it SARS-CoV-2. Nat Microbiol 5(4): 536–544.

Guebre-Xabier M, Patel N, Tian JH, *et al*., 2020. NVX-CoV2373 vaccine protects cynomolgus macaque upper and lower airways against SARS-CoV-2 challenge. Vaccine 38(50): 7892–7896.

Guo Y, Dong Y, Zheng R, *et al*., 2024. Correlation between viral infections in male semen and infertility: A literature review. Virol J 21: 167.

Hoffmann M, Kleine-Weber H, Schroeder S, *et al*., 2020. SARS-CoV-2 cell entry depends on ACE2 and TMPRSS2 and is blocked by a clinically proven protease inhibitor. Cell 181(2): 271–280.

Javadzadeh M, Moghadam FR, Erfanifar E, *et al*., 2024. Evaluation of female infertility and viral diseases: A systematic review of coronaviruses. Sex Disabil 42(4): 567–589.

Jiang RD, Liu MQ, Chen Y, *et al*., 2020. Pathogenesis of SARS-CoV-2 in transgenic mice expressing human angiotensin-converting enzyme 2. Cell 182(1): 50–58.

Kruglov AA, Bondareva MA, Gogoleva VS, *et al.* 2024. Inactivated whole virion vaccine protects K18-hACE2 Tg mice against the Omicron SARS-CoV-2 variant via cross-reactive T cells and nonneutralizing antibody responses. Eur J Immunol. 54(3): e2350664.

Kozlovskaya LI, Piniaeva AN, Ignatyev GM, *et al.* 2021. Long-term humoral immunogenicity, safety and protective efficacy of inactivated vaccine against COVID-19 (CoviVac) in preclinical studies. Emerg Micro Infec 10(1): 1790-1806.

Lelis F, Byk LA, Pustylnikov S, *et al*., 2023. Safety, immunogenicity and efficacy of an mRNA-based COVID-19 vaccine, GLB-COV2-043, in preclinical animal models. Sci Rep 13: 21172.

Li Z, Xiang T, Liang B, *et al*., 2021. Characterization of SARS-CoV-2-Specific humoral and cellular immune responses induced by inactivated COVID-19 vaccines in a real-world setting. Front Immunol 12: 802858.

Liu J, Budylowski P, Samson R, *et al.*, 2022. Preclinical evaluation of a SARS-CoV-2 mRNA vaccine PTX-COVID19-B. Sci Adv 8(3): eabj9815.

Lu J, Tan S, Gu H, *et al*., 2024. Effectiveness of a broad-spectrum bivalent mRNA vaccine against SARS-CoV-2 variants in preclinical studies. Emerg Micro Infec 13(1): 2321994.

MacDonald NE, and SAGE Working Group on Vaccine Hesitancy, 2015. Vaccine hesitancy: Definition, scope and determinants. Vaccine 33(34): 4161–4164.

Muñoz-Fontela C, Dowling WE, Funnell SGP, *et al*., 2020. Animal models for COVID-19. Nature 586(7830): 509–515.

Munshi I, Khandvilkar A, Chavan SM, *et al*., 2021. An overview of preclinical animal models for SARS-CoV-2 pathogenicity. Indian J Med Res 153(1 & 2):17-25.

Nyberg T, Twohig KA, Harris RJ, *et al*., 2021. Risk of hospital admission for patients with SARS-CoV-2 variant B.1.1.7: Cohort analysis. BMJ 373: n1412.

Oladunni FS, Park JG, Pino PA, *et al*. 2020. Lethality of SARS-CoV-2 infection in K18 human angiotensin-converting enzyme 2 transgenic mice. Nat Commun 11 (1): 6122.

Onen EA, Sonmez K, Yildirim F, *et al*., 2022. Development, analysis, and preclinical evaluation of inactivated vaccine candidate for prevention of COVID-19 disease. All Life 15(1): 771-793.

Patone M, Handunnetthi L, Saatci D, *et al*., 2021. Neurological complications after first dose of COVID-19 vaccines and SARS-CoV-2 infection. Nat Med 27(12): 2144–2153.

Patone M, Thomas K, Hatch R, *et al*., 2021. Mortality and critical care unit admission associated with the SARS-CoV-2 lineage B.1.1.7 in England: An observational cohort study. Lancet Infect Dis 21(11): 1518–1528.

Sun SH, Chen Q, Gu HJ, *et al*., 2020. A mouse model of SARS-CoV-2 infection and pathogenesis. Cell Host Microbe 28(1): 124–133.

Suthar M, Manning KE, Ellis ML, *et al*., 2025. The KP.2-adapted COVID-19 vaccine improves neutralising activity against the XEC variant. Lancet Infect Dis 25 (3): e122-e123.

Tanriover MD, Doğanay HL, Akova M, *et al*. 2021. Efficacy and safety of an inactivated whole-virion SARS-CoV-2 vaccine (CoronaVac): interim results of a double-blind, randomised, placebo-controlled, phase 3 trial in Turkey. Lancet 398(10296): 213-222.

Ulbegi PH, 2023. Comparison of mouse species in an in vivo SARS-CoV-2 challenge model. Kafkas Univ Vet Fak Derg 29 (6): 689-695.

Vogel AB, Kanevsky I, Che Y, *et al*., 2021. BNT162b vaccines protect rhesus macaques from SARS-CoV-2. Nature 592(7853): 283–289.

Winkler ES, Bailey AL, Kafai NM, *et al*., 2020. SARS-CoV-2 infection of human ACE2-transgenic mice causes severe lung inflammation and impaired function. Nat Immunol 21(11): 1327-1335.

Wu Z, Hu Y, Xu M, *et al*., 2021. Safety, tolerability, and immunogenicity of an inactivated SARS-CoV-2 vaccine (CoronaVac) in healthy adults aged 60 years and older: a randomised, double-blind, placebo-controlled, phase 1/2 clinical trial. Lancet Infect Dis 21(6): 803-812.

Yinda CK, Port JR, Bushmaker T, *et al*., 2021. K18-hACE2 mice develop respiratory disease resembling severe COVID-19. PLoS Pathog 17(1): e1009195.

Yu J, Tostanoski LH, Peter L, *et al*., 2020. DNA vaccine protection against SARS-CoV-2 in rhesus macaques. Science 369(6505): 806–811.

Zhang Y, Zeng G, Pan H, *et al*. 2020. Safety, tolerability, and immunogenicity of an inactivated SARS-CoV-2 vaccine in healthy adults aged 18–59 years: a randomised, double-blind, placebo-controlled, phase 1/2 clinical trial. Lancet Infect Dis 21(2): 181-192.

In-Press